Electronic Doppler effect in resonant Auger decay of CO molecules upon excitation near a shake-up Π resonance

S. L. Sorensen,[1] M. Kitajima,[2,*] T. Tanaka,[2] M. Hoshino,[2] H. Tanaka,[2] Y. Tamenori,[3] R. Sankari,[4] M. N. Piancastelli,[5] K. Ueda,[6,†] Y. Velkov,[7,‡] I. Minkov,[7] V. Carravetta,[6,8] and F. Gel'mukhanov[6,7,§]

[1]*Department of Synchrotron Radiation Research, Institute of Physics, University of Lund, Box 118, SE-221 00 Lund, Sweden*

[2]*Department of Physics, Sophia University, Tokyo 102-8554, Japan*

[3]*Japan Synchrotron Radiation Research Institute, Sayo-gun, Hyogo 679-5198, Japan*

[4]*Department of Physics, Materials Science, University of Turku, Finland*

[5]*Department of Physics, Uppsala University, Box 530, SE-751 21 Uppsala, Sweden*

[6]*Institute of Multidisciplinary Research for Advanced Materials, Tohoku University, Sendai 980-8577, Japan*

[7]*School of Biotechnology, Royal Institute of Technology, S-106 91 Stockholm, Sweden*

[8]*Istituto per i Processi Chimico-Fisici, Area della Ricerca del CNR, via G. Moruzzi 1, I-56124 Pisa, Italy*

(Received 5 October 2007; published 14 December 2007)

We present an experimental observation of the electronic Doppler effect in resonant Auger spectra upon core excitation slightly above the carbon *K* edge of the CO molecule. Thus the electronic Doppler effect has been identified in above-threshold excitation, and in a transition of Π symmetry. *Ab initio* calculations of the potential energy curves of the relevant states of CO and the wave packet technique have been employed to provide a theoretical background to the experimental studies. The weak feature around 299.4 eV in the photoabsorption spectrum, whose decay has been investigated by the present experiment, is assigned to double (core-valence) excitations to C 1*s* shake-up states $|1s_C^{-1}1\pi^{-1}\pi^{*2}\rangle$ with a strong dissociative character, and the Doppler splitting of the atomic peak has been reproduced by the simulation.

DOI: 10.1103/PhysRevA.76.062704 PACS number(s): 32.80.Hd, 33.20.Rm, 33.60.Fy

I. INTRODUCTION

The ability to follow nuclear dynamics in molecules on an ultrashort time scale has developed in several directions, where direct pump-probe studies or core-level spectroscopy can reveal femtosecond or even attosecond dynamics in atoms and molecules. Although both methods are highly successful, there are limitations on the information obtained about the temporal or the energetic parameters from a single measurement. X-ray scattering offers a highly sensitive spectroscopic tool which reflects the temporal dynamics through the electronic transitions studied using high-resolution core-level spectroscopies [1–4]. Many new dynamical processes have been discovered and explained since the advent of the x-ray Raman scattering methods allowing investigation of dynamical effects on the femtosecond time scale.

Core electrons may be excited to either bound or dissociative states; the subsequent decay processes can be successfully studied using multicoincidence techniques [3,5] or resonant Auger scattering (RAS) [1–4]. As dissociative core-excited states are relatively common in a wide range of molecules, studying their dynamical properties has a self-evident importance.

The RAS spectral band consists of two qualitatively different subbands, related either to decays near the equilibrium geometry (molecular band) or to decays in the dissociation region of the electronic-state potential surface, far from equilibrium. When a fragment of the dissociation is a core-excited atom, the decays in the dissociation region form a narrow, nondispersive resonance, which is known as the atomic, or dissociative, peak [1,2]. After the discovery of the atomic peak [6], it was recognized that this resonance can be strongly affected by an electronic Doppler effect arising from the velocity of the excited atomic fragment [1,7]. The atomic Auger peak can be Doppler broadened or even split [8–14]. The Doppler splitting is usually about 0.5–1 eV, depending primarily on the kinetic energy release upon molecular dissociation, the momentum of the Auger electron, and the angle between the velocity vector of the fragment and the measurement direction. Under proper conditions, the Doppler effect for Σ transitions involving 1*s* electrons is relatively easy to identify with sufficient resolution and angle-resolved detection. This effect has proven to be a powerful tool in studies of the dynamics of ultrafast dissociation [2,4,5,10,14–16]. Until now, all Doppler experiments have been performed for core excitations to unoccupied σ molecular orbitals.

In this study we present an experimental and theoretical investigation of the electronic Doppler effect upon double (core-valence) excitation to a core shake-up state of Π symmetry. The observed (≈0.6 eV) Doppler splitting constitutes direct proof that this state is dissociative. The photon-energy-dependent measurements allow us to identify the energetic spread of the dissociative state, and the kinetic energy of the Doppler-shifted electron provides information about the excited-state potential surface.

The paper is organized as follows. In the next section we describe the experimental details. In Sec. III, we present ex-

*Present address: Department of Chemistry, Tokyo Institute of Technology, Tokyo 152-8551, Japan.

†ueda@tagen.tohoku.ac.jp

‡yasve@theochem.kth.se

§On leave from Institute of Automation and Electrometry, 630090 Novosibirsk, Russia.

perimental results. Section IV presents the theoretical approach used in this investigation. Section V outlines more specifically the computational details. We compare and discuss experimental and theoretical results in Sec. VI. Finally, our findings are summarized in Sec. VII.

II. EXPERIMENTAL DETAILS

The experimental study was carried out at the 27SU [17,18] figure-8 undulator beamline at the Japanese 8-GeV synchrotron radiation laboratory SPring-8. The polarization vector **e** of the undulator light may be set to horizontal (first harmonic) or vertical (0.5 harmonic) by tuning the undulator [19]. The electron spectra were measured using an electrostatic hemispherical electron-energy analyzer (Gammadata-Scienta SES2002) with the lens fixed perpendicular to the photon beam in the horizontal plane [20].

The monochromator band pass was set to ~70 meV full width at half maximum (FWHM), and the spectrometer broadening contributed an equal amount, resulting in a total experimental broadening of 100 meV in addition to a thermal Doppler broadening of about 40 meV. The symmetry-dependent ion-yield measurements were carried out with two identical energetic ion detectors [3,21] in a separate chamber mounted upstream of the electron analyzer chamber. The photon energy calibration was made using the ion-yield spectra measured with a total-ion-yield detector [3,21]. The sharp features near 301 eV are known from the study by Domke [22], with the most prominent peak at 300.69 eV, and could be used for calibration. In the C 1*s* ionization region, measurements of the photon flux by photocurrent suffer from carbon contamination on the surface of the optical components, and the photon flux reading was thus corrected by comparing intensities of angle-resolved Ar 2*p* photoelectron spectra with the known cross sections and angular distributions at the photon energy of interest [23,24]. The sample of carbon monoxide gas was commercially obtained with a purity of >99.99%.

III. EXPERIMENTAL RESULTS

A. Carbon 1*s* symmetry-resolved ion-yield spectra

The symmetry-resolved C 1*s* near-edge ion-yield spectrum is presented in Fig. 1. The spectral components corresponding to perpendicular Π transitions and parallel Σ transitions are shown separately in the plot, and a spectrum representing the total ion yield is included in the plot. The discrete doubly excited states were measured by Shaw *et al.* using electron-energy loss in 1984 [25], and later by Domke *et al.* [22], Ma *et al.* [26], and Köppe *et al.* [27]. The configuration of these states was not identified in these earlier studies, but it was generally agreed that the most likely configuration is the C $1s$-π^* excitation accompanied by a 1π or 5σ electron shake-up to an $nl\lambda$ Rydberg state. Ma identified at least four different vibrational progressions in this region by comparison of different isotopic spectra [26].

The experimental perpendicular component of the x-ray absorption spectrum (Π channel in Fig. 1) clearly shows a series of vibrational progressions within the doubly excited

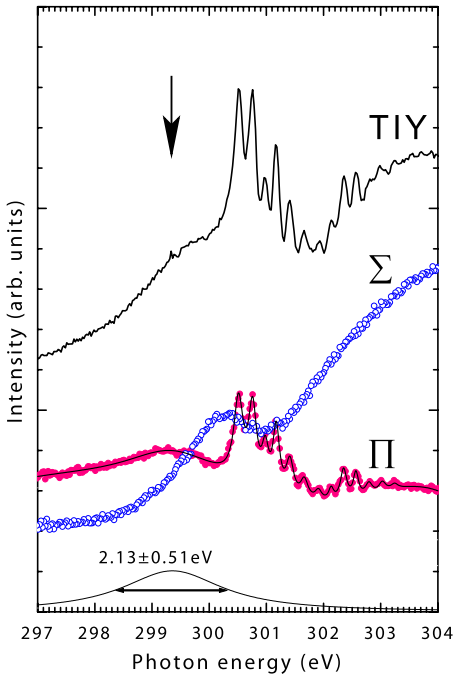

FIG. 1. (Color online) Experimental x-ray absorption of CO: total ion yield (TIY) and components with Π and Σ symmetry. The arrow indicates the feature studied in this paper. The Π channel was fitted, and the resulting profile for the 2.13 eV broad resonance centered at 299.5 eV is shown.

states. These states were addressed first theoretically by Ågren and Arneberg and identified as shake-up transitions associated with C $1s \rightarrow \pi^*$ excitation [28]. In the study by Köppe *et al.* [35], the decay from these doubly excited states was measured as a vibrational enhancement of the CO C 1*s* photoelectron spectrum [27]. In that work they simulated the first progression modeled by a harmonic potential. The resulting simulation reproduced the measured Franck-Condon factors approximately.

The ion-yield measurements by Stolte *et al.* [29] clearly reveal not only the discrete states above 300 eV, and the shape resonance feature extending up to 310 eV, but in the CO^{2+} yield a broad feature visible at 299.5 eV. This feature is also visible in the spectra in Refs. [27,30], but was not studied directly in these papers. We find that this spectral feature consists of two broad peaks, one in the Π transition and the other in the Σ transition, as seen in Fig. 1. The result of a least-squares curve fitting of the Π spectrum is included in the plot. The main focus of the rest of the paper is to study the electronic decay from this broad feature at ~299.4 eV [width (FWHM) of 2.13±0.51 eV] in the Π channel. We will show that calculation together with the experimental Auger spectra allows us to assign this feature to C 1*s* shake-up states $|1s_C^{-1}1\pi^{-1}\pi^{*2}\rangle$ of Π symmetry.

B. Resonant electronic decay spectra

The electron spectra of carbon monoxide have been recorded at photon energies in the range between 298.6 and 300 eV for Auger electron emission in the directions parallel

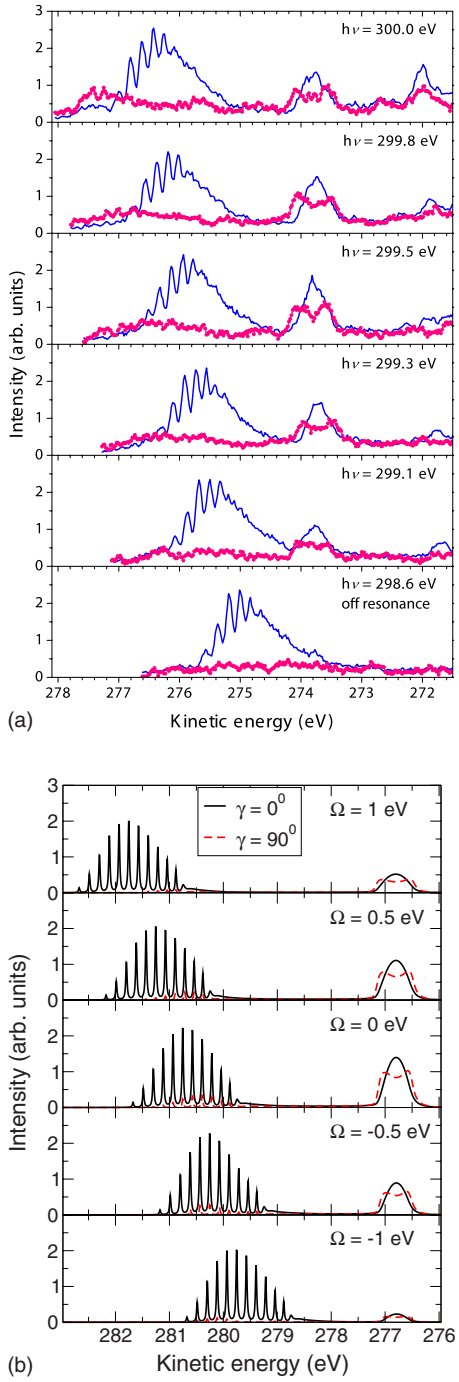

FIG. 2. (Color online) (a) Experimental RAS spectra of carbon monoxide for different excitation energies using an experimental setup with parallel (γ=0°, solid line) and perpendicular (γ=90°, dots) orientation of the Auger electron momentum relative to the light polarization vector $\gamma = \angle \mathbf{e},\mathbf{p}$. (b) Calculated RAS spectra of carbon monoxide for the measurement geometries; $\gamma = \angle \mathbf{e},\mathbf{p}$ =0°,90°, and parameters $\Omega = \omega 301.7$ eV, A=430 a.u.

and perpendicular to the light polarization vector **e**. For later convenience we introduce here the angle γ between the Auger emission with momentum **p** and the light polarization vector **e**, $\gamma = \angle \mathbf{e},\mathbf{p}$. The spectra in the 270–277 eV kinetic energy range are presented in Fig. 2(a), where the solid and dotted lines represent the spectra at γ=0° and 90°, respectively. This kinetic energy range would roughly correspond to the 22–28 eV binding-energy range, but as the photon energy is tuned over a 1.5 eV range, the binding-energy range shifts in each spectrum.

In the "parallel" spectra at γ=0°, there is a rather intense feature which has a partially resolved vibrational progression. It seems fairly clear from the behavior of the intensity of this feature as the photon energy is scanned through the resonance that direct photoionization is responsible for this feature. The relative intensities of the peaks are more or less unchanged in each spectrum, and the dispersion of the peaks is as expected for molecular ionic states. Our 298.6 eV spectra can thus be considered to represent the direct photoionization and the anisotropy parameter β for the direct photoionization of this band is ~2.

According to a high-resolution photoelectron study by Baltzer *et al.* [31], there are two overlapping bound electronic states, $3\,^2\Sigma^+$ and $D\,^2\Pi$, which are responsible for this feature. The $3\,^2\Sigma^+$ state with a $5\sigma^{-1}1\pi^{-1}\pi^*$ configuration has an adiabatic peak at 22.993 eV [31]. We can clearly identify this 0-0 peak at 277 eV in our 300 eV spectrum (top panel). In the high-resolution photoelectron spectrum by Baltzer *et al.* [31], this state exhibits a long vibrational progression with 13 peaks, whose vibrational spacing is ~200 meV for the lowest levels but decreases very rapidly, due to strong anharmonicity, to 116 meV for the ν=5 and 6 levels. Thus, we can attribute the observed vibrational progression to that of the $3\,^2\Sigma^+$ state: as our experimental resolution is ~130 meV, we are not able to resolve the higher vibrational peaks. Baltzer *et al.* found also that the $3\,^2\Sigma^+$ state has β values of 0.7–1.7 in the photon energy range 36–44 eV [31]. The difference in the β values may be attributed to the difference in the photon energies employed in the present experiment (soft x ray) and those in [31] (vacuum ultraviolet).

The $D\,^2\Pi$ state, with leading configurations $5\sigma^{-2}\pi^*$ and $4\sigma^{-1}5\sigma^{-1}\pi^*$, on the other hand, begins a progression at 22.378 eV binding energy, i.e., 276.2 eV in our 298.6 eV direct photoionization spectra (bottom panel). Although this state also exhibits a clear vibrational progression in the high-resolution study, we can barely discern the vibrational structure attributable to this band in our spectra. Baltzer *et al.* found β values close to 0 for this state [31] and thus in principle this state is expected to be populated in both parallel (γ=0°) and perpendicular (γ=90°) spectra. In our direct photoionization spectrum (bottom panel), the D state is very weak, but the intensity below the onset of the $3\,^2\Sigma^+$ state appears to increase at higher photon energies and may be attributed to the D state.

There is another final state that was identified by Baltzer *et al.* and is visible in our spectra. The $3\,^2\Pi$ state with a leading $4\sigma^{-1}5\sigma^{-1}\pi^*$ configuration has a repulsive potential in the Franck-Condon region [31]. It appears at 27.4 eV binding energy but is a relatively broad peak, and the peak width seems to vary with photon energy. It is probably responsible for the peak that moves steadily to higher kinetic energy in our spectra, resulting in a clear peak at 272 eV in the 300 eV spectrum (top panel), and a weaker peak at slightly higher energy.

There is one more prominent peak at kinetic energy of 273.8 eV in the measured spectra in Fig. 2(a). This peak is

not visible in the 298.6 eV direct photoionization spectrum, but has significant intensity in the other spectra. The peak remains fixed at kinetic energy ~274.2 eV, and has a very different overall profile in the parallel ($\gamma=0°$) and perpendicular ($\gamma=90°$) spectra. This behavior is typical of the Doppler split atomic Auger peak. The Doppler splitting, however, appears in the perpendicular ($\gamma=90°$) spectra, whereas in earlier studies the Doppler splitting always appeared in the parallel ($\gamma=0°$) spectra [8–14]. The reason that the Doppler splitting appears in the perpendicular ($\gamma=90°$) spectra is because the dissociative core-excited state that undergoes ultrafast fragmentation has Π symmetry. We tentatively identify the final state of this electronic transition as the dissociation limit of the $3\ ^2\Sigma^+$ ($5\sigma^{-1}1\pi^{-1}\pi^*$) state. We will discuss this point later.

IV. THEORY

The electronic Doppler effect has been used to study ultrafast dissociation in several molecules for excitation of $1s$ electrons in oxygen and fluorine to dissociative states of Σ symmetry [8,9,12]. The present study focuses on the excitation of carbon $1s$ electrons into a dissociative state of Π symmetry. In order to illustrate the role of the symmetry of the core-excited state, we consider excitation to dissociative states of Σ and Π symmetry in parallel. The peak shapes and the effect of the dynamical parameters are discussed.

A. Qualitative picture of the Doppler splitting

Although molecules in the gas phase are randomly oriented, the absorption of a photon with polarization **e** is essentially an anisotropic process, as the absorption probability is proportional to $|\mathbf{e}\cdot\mathbf{d}|^2$, where **d** is the transition dipole moment. Thus molecules that are aligned either perpendicular or parallel to **e** are preferentially excited for electronic transitions of type $1s\rightarrow\pi^*$ or $1s\rightarrow\sigma^*$ [see Fig. 3(a) for CO].

This implies that the velocity vector **v** of the dissociating carbon atom is preferentially perpendicular to **e** for Π or parallel for Σ excitations. For dissociation where kinetic energies of a few electron volts are released, the velocity **v** of the excited fragment and the momentum **p** of the Auger electron can lead to a substantial electronic Doppler shift $\mathbf{v}\cdot\mathbf{p}$. As the probability for parallel and antiparallel molecular orientations is equal, the decay from a dissociative potential is Doppler split in two components for the two cases: $\mathbf{p}\perp\mathbf{e}$ for a Π excitation, and $\mathbf{p}\|\mathbf{e}$ for a Σ excitation [Fig. 3(a)].

We present a simplified theory of the Doppler effect in RAS. In a two-step model the Auger process is initiated by absorption of a photon of frequency ω near the ground-state equilibrium geometry R_0, followed by ejection of an Auger electron with energy $E=p^2/2$, with $p=|\mathbf{p}|$. Immediately after the core excitation from the ground state, the molecule in the core-excited state starts to decay to the final state. Decay transitions close to R_0 form a molecular band, while the atomic, or dissociative, peak is formed by decay in the dissociative region, $R\approx v/\Gamma$. In this section, we assume that the lifetime of the core-excited state $1/\Gamma$ is sufficiently long to allow the molecule to approach the dissociative region,

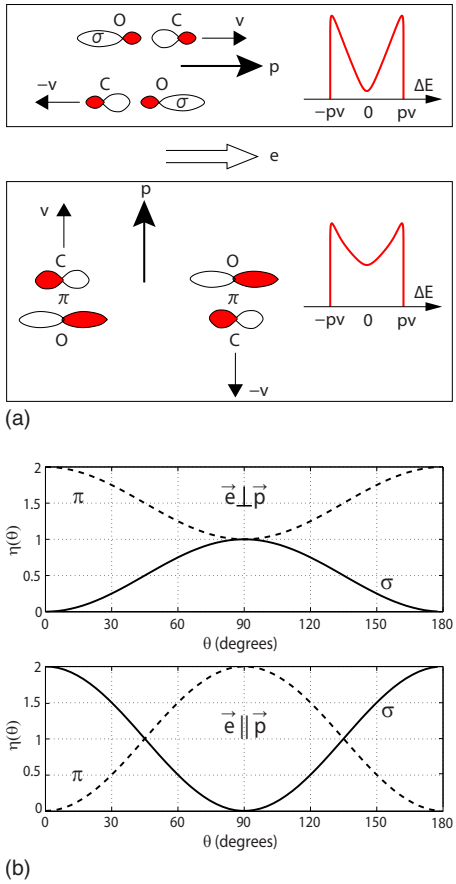

FIG. 3. (Color online) (a) Physical picture of Doppler splitting for $1s\rightarrow\sigma^*$ and $1s\rightarrow\pi^*$ excitations: the dissociative peak is Doppler split when $\mathbf{p}\|\mathbf{e}$ and $\mathbf{p}\perp\mathbf{e}$, respectively. (b) Anisotropy of $1s\rightarrow\sigma^*$ and $1s\rightarrow\pi^*$ photoexcitations.

where the potentials of the core-excited and of the final states are flat at $R=\infty$. The RAS cross section for randomly oriented diatomic molecules must be integrated over all orientations. The spectral shape of the dissociative (or atomic) peak is a convolution of the core-excitation [$\propto\eta(\theta)$] and the decay probabilities [9]:

$$\sigma(E,\omega)\propto\int_0^\pi d\theta\sin\theta\frac{\eta(\theta)|q(\theta,R)|^2}{(\Delta E-pv\cos\theta)^2+\Gamma^2}. \qquad (1)$$

Here, $\theta=\angle\mathbf{v},\mathbf{p}$ is the angle between the direction of the ejected Auger electron and the molecular axis; $\Delta E=E-\omega_{cf}(\infty)$, with $\omega_{cf}(\infty)$ being the difference between the potential curves of the core-excited (c) and final (f) states in the dissociative region at $R=\infty$. We neglect the *angular anisotropy* of the amplitude of Auger decay, $q(\theta,R)$ [14], but we retain its R dependence. It should be noted that the Doppler effect can occur also for a bound core-excited state. However, in this case the potential curve of the final state must be parallel to that of the core-excited state [32].

We can estimate the magnitude of the Doppler shift of the atomic peak if we know the velocity of the dissociating core-excited fragment. In the case of a diatomic molecule, using

decay from a core-excited state at the C K edge of carbon monoxide as an example, the velocity is defined as

$$v = \frac{\sqrt{2\mu\epsilon}}{m_C}, \quad \epsilon = \Omega - \Delta E + \Delta \approx \Delta, \tag{2}$$

where $\mu = m_O m_C/(m_O + m_C)$ is the reduced mass of the CO molecule, $\Omega = \omega - [E_c(R_0) - E_0(R_0)]$, and $E_i(R)$ is the potential energy surface of the electronic state i $(i = 0, c, f)$. The kinetic energy release $\Delta = E_c(R_0) - E_c(\infty)$ is typically a few electron volts and is considerably larger than the thermal energy $k_B T \approx 0.03$ eV. This is the origin of the striking Doppler-splitting effect, which is visible with an experimental spectral resolution of several hundred meV when the angular condition is satisfied.

The decay probability, given by the Lorentzian in Eq. (1), produces a homogeneous distribution of Doppler-shifted resonances over the entire range of angles $0° \leqslant \theta \leqslant 180°$. However, the anisotropy of the photoabsorption [9],

$$\eta(\theta) = \frac{1}{2}\begin{cases} 1 + \cos^2\theta + (\mathbf{e}\cdot\hat{\mathbf{p}})^2(1 - 3\cos^2\theta), & 1s \to \pi^*, \\ 2\cos^2\theta + [(\mathbf{e}\cdot\hat{\mathbf{p}})^2 - 1](3\cos^2\theta - 1), & 1s \to \sigma^*, \end{cases} \tag{3}$$

$\hat{\mathbf{p}} \equiv \mathbf{p}/p$ being a unit vector, has a serious impact on the Doppler profile. This can be easily demonstrated in the limit of a large Doppler shift, $pv \gg \Gamma$, where

$$\sigma(E, \omega) \propto \eta(\theta_{\text{res}}), \quad \cos\theta_{\text{res}} = \frac{\Delta E}{pv}, \tag{4}$$

when $|\Delta E| \leqslant pv$.

Figure 3(b) clearly demonstrates the anisotropy of the photoabsorption $\eta(\theta)$. Note the lack of core-excited fragments near $\theta = 90°$ for $\mathbf{e} \| \mathbf{p}$ and $1s \to \sigma^*$ excitation. A similar situation is found for the case $\mathbf{e} \perp \mathbf{p}$ for $1s \to \pi^*$ excitation. Such an "orientation hole" prevents molecules with a certain orientation from contributing to the total spectrum, and results in a Doppler splitting of the Auger peaks, given by Eq. (4), for the two cases shown in Fig. 3(a).

We would like to point out that the dip in $\eta(\theta)$ in the region $\theta = 90°$ is smaller for the Π excitation compared to the Σ excitation. This naturally leads to a more pronounced Doppler splitting for a Σ-type excitation, making the observation of Doppler-split fragment Auger lines in core excitation to Π states more difficult. This is one reason that the effect has not yet been identified for Π transitions.

B. Time-dependent theory of the electronic Doppler effect

We now focus on the strict theory of the Doppler effect in resonant Auger scattering. Equation (1) dictates that in order to obtain the RAS cross section of randomly oriented molecules, we need to integrate the cross section over all molecular orientations (angle θ):

$$\sigma(E, \omega) = \int_0^\pi \sigma(E, \omega, \theta) \sin\theta \, d\theta. \tag{5}$$

In a stationary representation, the nuclear wave functions must extend into the continuum region, as the Doppler effect is intrinsically connected to dissociative core-excited states [7]. As discussed earlier, the total RAS profile is formed through continuum-bound and continuum-continuum electronic decays. It is desirable to avoid continuum wave functions in numerical simulations to reduce computational costs. A solution is offered by the wave-packet technique [33,34]. The superior performance of the wave-packet method, especially in cases where dissociative states are involved, makes it the theoretical method of choice for performing resonant Auger scattering simulations.

The RAS cross section of fixed-in-space molecules can be written in the time-dependent representation as a half Fourier transform

$$\sigma(E, \omega, \theta) = \text{Re} \int_0^\infty d\tau \, \sigma(\tau) e^{\imath(\omega - E + \imath\Gamma_f)\tau} \tag{6}$$

of the autocorrelation function

$$\sigma(\tau) = |A|^2 \sigma_{\text{dir}}(\tau) + (\mathbf{e}\cdot\mathbf{d}_{c0})^2 \sigma_{\text{res}}(\tau) + (\mathbf{e}\cdot\mathbf{d}_{c0}) \sigma_{\text{int}}(\tau),$$

$$\sigma_{\text{dir}}(\tau) = \langle 0 | \varphi_f(\tau) \rangle, \quad \sigma_{\text{res}}(\tau) = \langle \Psi(0) | \Psi(\tau) \rangle,$$

$$\sigma_{\text{int}}(\tau) = \imath\{A \langle \Psi(0) | \varphi_f(\tau) \rangle - A^* \langle 0 | \Psi(\tau) \rangle\},$$

which is the sum of the direct and resonant contributions and of the term $\sigma_{\text{int}}(\tau)$ which describes the interference between direct and resonant scattering. The dynamics of the resonance and interference scattering depend on the wave packets propagating in the final and core-excited electronic states,

$$|\varphi_f(t)\rangle = e^{-\imath(H_f - E_0)t} |0\rangle,$$

$$|\Psi(\tau)\rangle = e^{-\imath(H_f - E_0)\tau} |\Psi(0)\rangle,$$

$$|\Psi(0)\rangle = Q(\theta, R) \int_0^\infty dt \, e^{(\imath(\omega + E_0 - H_c) - \Gamma)t} |0\rangle.$$

Here H_c and H_f denote the nuclear Hamiltonians of the core-excited and final states, and $E_0 = E_0(R_0) + \omega_0/2$ with ω_0 being the ground-state vibrational frequency. The formal origin of the Doppler effect is the phase factor in the Auger decay amplitude [1,7]:

$$Q(\theta, R) = q(\theta, R) e^{\imath\alpha p R \cos\theta}, \quad \alpha = \mu/m_C. \tag{7}$$

Here we neglect the anisotropy of the decay amplitude

$$q(\theta, R) \approx q(R). \tag{8}$$

One should keep in mind that this phase factor originates from the wave function of the Auger electron emitted in the vicinity of the dissociating core-excited atom (in the present case, carbon).

It is straightforward to see that the interference term is equal to zero,

$$\sigma_{\text{int}}(\tau) = 0, \tag{9}$$

for a core-excited state of π symmetry. Averaging the interference term $\sigma_{\text{int}}(\tau) \propto (\mathbf{e} \cdot \mathbf{d}_{c0})$ over all orientations of the $\mathbf{d}_{c0}$ about the molecular axis we find that the terms cancel since $\mathbf{d}_{c0}$ is perpendicular to the molecular axis.

The measurement in Fig. 2(a) shows a strong anisotropy in the direct channels $(5\sigma, 1\pi \rightarrow \psi_{\mathbf{p}}, \pi^*)$ arising from the transition dipole moment for direct photoionization $A \propto (\mathbf{e} \cdot \mathbf{d}_{f0})$. Indeed, the comparison of the two scattering geometries $\gamma = 0°, 90°$ for large detunings shows that the cross section of the direct channel is almost completely suppressed for $\gamma = 90°$. Thus in our simulations the intensity of the direct channels is taken proportional to $\cos^2 \gamma$, thus replacing $|A|^2$ by $|A|^2 \cos^2 \gamma$. Now we are in a position to write down the final expression for the autocorrelation function averaged over all orientations of $\mathbf{d}_{c0}$:

$$\sigma(\tau) = |A|^2 \cos^2 \gamma \sigma_{\text{dir}}(\tau) + \eta(\theta) \sigma_{\text{res}}(\tau), \tag{10}$$

where $\eta(\theta)$ is defined in Eq. (3).

V. COMPUTATIONAL DETAILS

A. Potential curves

In order to analyze the photoabsorption spectrum of CO slightly above the C K edge, in particular the small shoulder in the spectrum of Π character at ~299.4 eV (see Fig. 1), we have carried out multireference configuration interaction (MRCI) calculations by using the CIPSI (configuration interaction by perturbation with multiconfigurational zeroth-order wave function selected by an iterative process) method with aimed selection [35,36]. The application of a variational approach to the calculation of a highly excited quasistationary state near the ionization threshold presents some technical difficulties due to the possible energetic collapse of the state and the merging of the quasistationary state with a large number of Rydberg and electronic continuum states. These two problems have been efficiently taken into account by the CI approach, which allows for a convenient selection of the electronic configurations to include in the calculation, and by the projection on a medium size basis set: GAMESS-PVTZ, $(10s, 6p, 1d) \rightarrow [5s, 3p, 1d]$ [37], giving a limited representation of Rydberg and continuum orbitals. The same computational technique has been employed for the calculation of the other molecular states involved in the resonant Auger decay.

MRCI calculations have been carried out at 18 different geometries in the range $R = 1.80$–4.0 a.u., around the equilibrium geometry ($R_0 = 2.132$ a.u.) of the ground state, in order to estimate the adiabatic potential curves. A unique CI space was used for all geometries in order to avoid discontinuities in the potential energy curves. This determinantal space is the union of the CI spaces selected at some of the considered internuclear distances; this strategy has proven to give a balanced treatment for different states and different internuclear distances. Ten C $1s$ core-excited states of Π_x symmetry have been computed in this way; only the lowest six states will be discussed in detail in the following. They are characterized by a dominating contribution of one or two

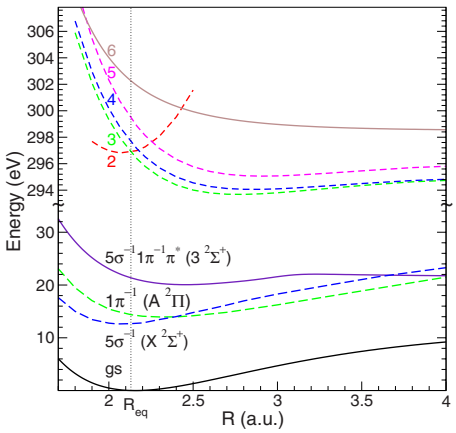

FIG. 4. (Color online) Calculated potential energy surfaces of CO. Solid lines, potentials used in our simulations of the resonant Auger spectral profile, by wave-packet dynamics; dashed lines, other electronic states with reference purposes only. Main contributions in the plotted core-excited states are as follows: 2, $1s_C^{-1}1\pi^{\text{Ryd}}$; 3, 5, 4, 6, $1s_C^{-1}1\pi^{-1}\pi^*\pi^*$.

of the following five configurations: $a = 1s_C^{-1}\pi_x^*$, $b = 1s_C^{-1}\pi_x^{\text{Ryd}}$, $c = 1s_C^{-1}1\pi_x^{-1}\pi_x^{*2}$, $d = 1s_C^{-1}1\pi_x^{-1}\pi_y^{*2}$, $e = 1s_C^{-1}1\pi_y^{-1}\pi_x^*\pi_y^*$. The first two configurations correspond to single excitations to either the antibonding π^* or a Rydberg orbital, while the remaining three configurations correspond to double (shake-up) excitations also involving the valence orbital 1π. It should be noted that the last configuration (e), involving four open shells, may give rise to two distinct singlet spin-orbit configurations. A simple inspection of the larger CI coefficients of the six lowest computed core-excited states allowed an easy diabatization based on maintaining a specific combination of the electronic configurations a–e in the diabatic states, in order to isolate the diabatic excited Rydberg state. The resulting potential curve is shown in Fig. 4 as state 2. The potentials of states 3, 4, and 5 in the same figure are highly dissociative near the ground-state equilibrium geometry (with a very small minimum above $R = 2.5$ a.u.).

Our *ab initio* calculation suggests assignment of the 299.4 eV broad peak feature in the Π spectrum in Fig. 1 to a doubly excited shake-up state $|c\rangle = |1s_C^{-1}1\pi^{-1}\pi^{*2}\rangle$ of Π symmetry, that we identify as the state 6. The other core-excited shake-up states $|1s_C^{-1}1\pi^{-1}\pi^{*2}\rangle$ are also located below the bound shake-up states. All of these states are of strongly dissociative character, which is a prerequisite for Doppler-split atomic peaks in RAS spectra. Although these states could, in principle, contribute to the Doppler-split peak, the calculated excitation energy at the ground-state bond distance is far below the energy of state 6. In addition, state 6 is energetically isolated at ~4 eV above the ionization threshold, which agrees with the experimental peak (at ~299.4 eV in Fig. 1). States 3–6 have large contributions from doubly excited configurations, which generally leads to a low transition probability. In Fig. 5, we compare the theoretical profiles of X-ray absorption spectra (XAS) for states 6 and 5 with the experimental XAS profile. The agreement is reasonable in terms of the width: the experimental FWHM is

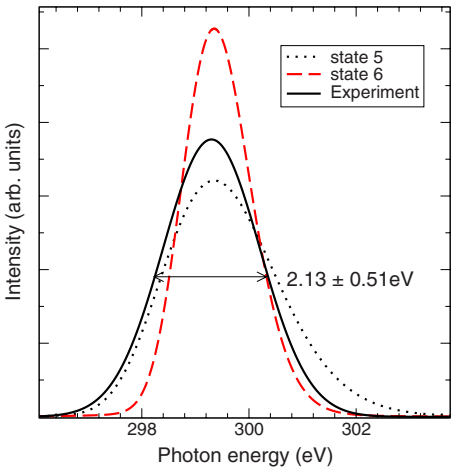

FIG. 5. (Color online) Theoretical XAS profiles of states 6 and 5 and the experimental XAS profile. The maxima of the theoretical spectra are shifted to the peak position of the experimental one. The same transition dipole moment for both states is assumed. Experimental FWHM is 2.13±0.51 eV. FWHM of state 6 is 1.50 eV and of state 5 is 2.47 eV.

2.13±0.51 eV while the calculated FWHMs of the states 6 and 5 is are 1.50 eV and 2.47 eV, respectively.

The Rydberg state 2 crosses the state of our interest, state 6, at about $R \approx 2.5$ a.u., and these states may interact each other at the crossing point. However, this interaction is very weak because it involves a single (2) and a double (6) core-excited state.

B. Wave-packet dynamics

We assume that the resonant scattering process terminates with an electronic transition from the core-excited state 6 to the final ionic state $|f\rangle = |1\pi^{-1}5\sigma^{-1}\pi^{*}\rangle$. Although there are several final states in the same energy region, Auger transition from the $|1s_{\mathrm{C}}^{-1}1\pi^{-1}\pi^{*2}\rangle$ core-excited state to many final states is forbidden. This is the case for the $|1\pi^{-1}\rangle$ and $|5\sigma^{-1}\rangle$ final states (Fig. 4). These states are populated only via direct photoionization. The $3\,^2\Sigma^+$ state $|1\pi^{-1}5\sigma^{-1}\pi^{*}\rangle$ has clearly distinguishable spectral lines and has substantial intensity in all of the observed spectra in Fig. 2(a), as already discussed. This state is included in the simulations of the spectra described below. The solid lines in Fig. 4 indicate the potential curves included in our model for the nuclear dynamics simulation.

The wave-packet simulations are based on a wave-packet code described elsewhere [38]. We used a value of $\Gamma = 0.032$ eV (HWHM) [39] for the lifetime broadening of the core-excited state and $d_{c0}=1$. The amplitude of the direct channel [38], $A=430$ a.u., was defined from fitting to the experimental RAS profile. The scheme of wave packet calculations outlined in Sec. IV B consists of three steps: (1) calculation of the autocorrelation function (10), (2) evaluation of the RAS cross sections given by Eq. (6) for a fixed-in-space molecule with a step $\Delta\theta=5°$, and (3) averaging of the cross section over molecular orientations relative to the momentum of the photoelectron as given by Eq. (5).

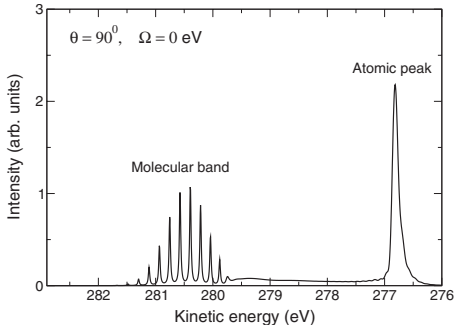

FIG. 6. RAS profile of fixed-in-space CO molecules for $q(R)$ =const. The contribution of the direct channel is neglected.

The experimental spectra depicted in Fig. 2(a) show strong anisotropy in the scattering, where the resonant contribution to the molecular band is relatively weak in the perpendicular geometry. The calculation, however, indicates that the resonant channel in the perpendicular geometry populates both the molecular band and the atomic peak in Fig. 6. The theory (Fig. 6) disagrees with the experiment [Fig. 2(a)] which shows a very weak molecular band at this angle. We believe that this may be due to the fact that the decay amplitude depends on the bond length, so that $q(R)$ is rather small near equilibrium geometry. We model this assumption using the following shape of the decay amplitude:

$$q(R) = 1 + \rho\left[\frac{1}{2} + \frac{1}{\pi}\arctan\left(\frac{R - R_c}{a}\right)\right]. \tag{11}$$

This model indeed results in a reduced amplitude for small R with respect to the dissociation region. The net effect is to increase the relative intensity of the atomic peak with respect to the molecular one. The decay amplitude was adjusted using $q(R)$: $\rho=3$ a.u., $R_c=2.9$ a.u., $a=0.4$ a.u.

In our model we consider the Auger decay from the double excited state C $1s^{-1}1\pi^{-1}\pi^{*2}$ to the final state $5\sigma^{-1}1\pi^{-1}\pi^{*}$. Assuming that the shake excitation $1\pi^{-1}\pi^{*}$ remains as "spectator" during the decay C $1s^{-1}1\pi^{-1}\pi^{*2} \rightarrow 5\sigma^{-1}1\pi^{-1}\pi^{*}\psi_{\mathbf{p}}$, the Auger amplitude depends on two-electron Coulomb integrals $[\psi_{\mathbf{p}}5\sigma|\pi^{*}1s_{\mathrm{C}}]$ and $[1s_{\mathrm{C}}5\sigma|\pi^{*}\psi_{\mathbf{p}}]$. To estimate these integrals it is sufficient to take into account the major one-center contribution, $[1s_{\mathrm{C}}5\sigma|\pi^{*}\psi_{\mathbf{p}}] \sim a_{5\sigma}a_{\pi^{*}}[1s_{\mathrm{C}}2p_{\mathrm{C}}|2p_{\mathrm{C}}\psi_{\mathbf{p}}]$, where $a_{5\sigma}$ and $a_{\pi^{*}}$ are the expansion coefficients that express the contributions from the atomic orbitals to the molecular orbitals; $5\sigma = a_{5\sigma}2p_{\mathrm{C}}+\cdots$ and $\pi^{*}=a_{\pi^{*}}2p_{\mathrm{C}}+\cdots$. Apparently the core-excited CO molecule behaves similarly to a valence-excited NO molecule $1\pi \rightarrow \pi^{*}$ which dissociates into neutral nitrogen and oxygen atoms. This means that in the region of dissociation we have three electrons in the $2p$ shell of core-excited carbon. Then the amplitude of the Auger decay in the dissociative region is $[1s_{\mathrm{C}}2p_{\mathrm{C}}|2p_{\mathrm{C}}\psi_{\mathbf{p}}]$, which is larger than the decay amplitude near equilibrium by a factor of $|a_{5\sigma}a_{\pi^{*}}|^{-1} \sim 4$, due to the fact that 5σ and π^{*} orbitals are equally delocalized over C and O for R close to R_0. This estimate is in agreement with our choice of the parameter $\rho=3$.

To conclude this section we list the approximations used in the current wave-packet simulations: (1) isotropy of the Auger decay amplitude $q(\theta,R)\approx q(R)$ as given by Eq. (8), (2) strong anisotropy of the direct channel $\sigma_{\mathrm{dir}}(E,\omega)\propto\cos^2\gamma$, (3) enhancement of the Auger decay in the dissociative region as given by Eq. (11), and (4) RAS cross sections computed for core-excited state 6 and final state $|1\pi^{-1}5\sigma^{-1}\pi^{*}\rangle$ (see Fig. 4).

VI. DISCUSSION

Now we are in a stage to discuss the results of the simulations and to compare them with the experiment.

A simultaneous analysis for the energy levels of the theoretical core-excited states (Fig. 4) together with the simulated XAS profile (Fig. 5) allows us to assign the core-excited state as $1s_{\mathrm{C}}^{-1}1\pi^{-1}\pi^{*2}$.

Both experiment [Fig. 2(a)] and theory [Fig. 2(b)] display a two-band structure of the RAS spectra. The first, lower-energy band (273.8 eV) is nondispersive. This is direct evidence that it is an atomic peak. In contrast, the broad high-energy band approximately follows the Raman dispersion law. The origin of this molecular band can be both direct photoionization and decay transitions near the equilibrium geometry. Both experiment and theory show that the spectral shape of the molecular band is insensitive to the photon energy. The intensity of the band does change slightly, but the main contribution is from the direct photoionization channel.

The experimental molecular band contains contributions from two different bound states: a main contribution comes from the $3\,^2\Sigma$ state, whereas a minor contribution from the $D\,^2\Pi$ state overlaps nearly completely in this region [31]. Our measurement in the x-ray region shows direct scattering into the $3\,^2\Sigma^+$ final state is strong, whereas that into the $D\,^2\Pi$ state is negligible [see the bottom panel of Fig. 2(a)]. Vibrational peaks above $\nu=5$ for the $3\,^2\Sigma$ state are not resolvable with our present resolution, but Baltzer's study resolves 12 peaks for the $3\,^2\Sigma$ state.

In the present theory, we included only $3\,^2\Sigma$ as a final state of RAS. Our calculated final-state potential also gives a vibrational progression up to the 12th vibrational level [Fig. 2(a)]. The simulated potential of the final $3\,^2\Sigma^+$ is, however, too steep near $R=3$ a.u. (Fig. 4), resulting in a lower anharmonicity.

The simulations nicely reproduce the existence of a quantitatively different anisotropy of the molecular band and atomic peaks [Fig. 2(a)]. The reason for it is that the molecular band is formed mainly due to direct photoionization which is strongly anisotropic in the studied high-energy region. The value of the anisotropy parameter β for ionization to $3\,^2\Sigma^+$ is ~ 2 in the presently investigated high-photon-energy region in contrast to value of $\beta\sim 1$ obtained earlier [31] for low photon energies $\omega=36,40,44$ eV.

The atomic peak has distinct characteristics. On the one hand, the atomic peak is due to transitions in the dissociative region, namely, to the Auger transition in an isolated core-excited carbon atom. In this case, due to the atomic spherical symmetry, the Auger scattering is almost isotropic ($\beta\approx 0$), i.e., the area of the atomic peak is almost the same for $\gamma=0°$ and 90°. On the other hand, we see a strong variation of the spectral profile of the atomic peak [Fig. 2(a)]. It is Doppler split when $\gamma=90°$, in contrast with the single peak seen in the parallel geometry. The theory [Fig. 2(b)] predicts a Doppler-broadened peak for $\gamma=0°$ and Doppler splitting ($2pv\approx 0.6$ eV) of the atomic peak when $\gamma=90°$ as observed in experimental spectra in Fig. 2(a). The wave-packet simulations confirm nicely the qualitative picture of the resonant Auger Doppler effect for a Π excitation (Sec. IV A).

The spacing (ΔE) between the atomic peak and the molecular band deserves some comment. The experimental value $\Delta E\approx 2$ eV is almost half the theoretical one, $\Delta E\approx 4$ eV. The origin of this disagreement is imperfection of the theoretical potentials of the core-excited and the final state since $\Delta E\approx E_6(R_{eq})-E_f(R_{eq})-[E_6(\infty)-E_f(\infty)]\approx 3.8$ eV is overestimated by the theory. For the same reason we observe a disagreement between the experimental and theoretical binding energies E_{bind}: the experimental binding energy of the first vibrational peak (22.99 eV) is nearly 3 eV higher than the calculated spectrum [Fig. 2(b), $\Omega=0$].

We should also comment on the final ionic state for the electronic decay. In our theoretical treatment, we have assumed that the final state of RAS is $3\,^2\Sigma^+$ with electronic configuration $5\sigma^{-1}1\pi^{-1}\pi^{*}$. The high-resolution photoelectron study [31] clearly shows that the $3\,^2\Sigma^+$ band ($E_{\mathrm{bind}}>23$ eV) and the $D\,^2\Pi$ band ($E_{\mathrm{bind}}>22.4$ eV) overlap in the energy region concerned. As we already noted, some intensity in the region $E_{\mathrm{bind}}<23$ eV appears in the RAS spectra in Fig. 2(a) ($\gamma=90°$) and can be attributed to the $D\,^2\Pi$ final state. These signals are absent in the direct scattering spectrum [the bottom panel of Fig. 2(a)]. Thus, the transition to the $D\,^2\Pi$ final state may be mostly attributed to the resonant scattering.

To conclude the discussion we would like to point out that the studied Auger spectra of CO molecule is illustrative for the importance of the Auger Doppler effect in studies of dissociative states. Moreover, we show that the anisotropy of the Auger Doppler effect gives direct information about the symmetry of the core-excited state (Π or Σ). Indeed, we see Doppler splitting for the orthogonal geometry in contrast with the case of σ core excitation [8,13,14], where the Doppler splitting occurs for $\gamma=0°$.

VII. CONCLUSIONS

We studied experimentally and theoretically the resonant Auger decay from a core-excited state of Π electronic symmetry. The investigation was performed on carbon monoxide, core-excited by a photon energy slightly above the carbon K edge. The experiment clearly displays Doppler splitting (0.6 eV) of the atomic peak for the orthogonal orientation of the Auger electron momentum relative to the polarization of the photon. The Auger resonance collapses to a single Doppler broadened peak for the parallel geometry. To explain the observed Doppler effect we computed potential surfaces for a number of shake-up states having the electronic configuration $|1s_{\mathrm{C}}^{-1}1\pi^{-1}\pi^{*2}\rangle$ and found the strong

dissociative behavior that is the prerequisite for an ultrafast dissociation and the Doppler splitting of the atomic peaks. The RAS spectra were simulated by wave-packet dynamics on the computed potential surfaces. Both experiment and theory display a strong anisotropy of the molecular band. The reason behind this is the significant contribution coming from direct photoionization, which is completely quenched for the orthogonal geometry. The set of experimental results is described quantitatively in the framework of the dynamical theory of the resonant Auger effect based on the wave-packet technique.

ACKNOWLEDGMENTS

The experiments were carried out with the approval of JASRI and supported in part by Grants-in-aid for Scientific Research from the Japanese Society for the Promotion of Science. We are grateful to the staff of SPring-8 for assistance during the measurements. S.L.S., Y.V., I.M., and F.G. acknowledge support from the Swedish Research council (VR) and the STINT foundation. F.G. and V.C. acknowledge support and hospitality from Tohoku University during their stay in Japan.

[1] F. Gel'mukhanov and H. Ågren, Phys. Rep. **312**, 91 (1999).
[2] S. L. Sorensen and S. Svensson, J. Electron Spectrosc. Relat. Phenom. **114-116**, 1 (2001).
[3] K. Ueda, J. Phys. B **36**, R1 (2003).
[4] K. Ueda, J. Phys. Soc. Jpn. **75**, 032001 (2006).
[5] K. Ueda and J. H. D. Eland, J. Phys. B **38**, S839 (2005).
[6] P. Morin and I. Nenner, Phys. Rev. Lett. **56**, 1913 (1986).
[7] F. Gel'mukhanov, H. Ågren, and P. Sałek, Phys. Rev. A **57**, 2511 (1998).
[8] O. Björneholm, M. Bässler, A. Ausmees, I. Hjelte, R. Feifel, H. Wang, C. Miron, M. N. Piancastelli, S. Svensson, S. L. Sorensen, F. Gel'mukhanov, and H. Ågren, Phys. Rev. Lett. **84**, 2826 (2000).
[9] A. Baev, F. Gel'mukhanov, P. Sałek, H. Ågren, K. Ueda, A. de Fanis, K. Okada, and S. Sorensen, Phys. Rev. A **66**, 022509 (2002).
[10] O. Björneholm, J. Chem. Phys. **115**, 4139 (2001).
[11] L. Rosenqvist, K. Wiesner, A. Naves de Brito, M. Bässler, R. Feifel, I. Hjelte, C. Miron, H. Wang, M. N. Piancastelli, S. Svensson, O. Björneholm, and S. L. Sorensen, J. Chem. Phys. **115**, 3614 (2001).
[12] K. Wiesner, A. Naves de Brito, S. L. Sorensen, F. Burmeister, M. Gisselbrecht, S. Svensson, and O. Björneholm, Chem. Phys. Lett. **354**, 382 (2002).
[13] K. Ueda, M. Kitajima, A. De Fanis, T. Furuta, H. Shindo, H. Tanaka, K. Okada, R. Feifel, S. L. Sorensen, H. Yoshida, and Y. Senba, Phys. Rev. Lett. **90**, 233006 (2003).
[14] M. Kitajima, K. Ueda, A. De Fanis, T. Furuta, H. Shindo, H. Tanaka, K. Okada, R. Feifel, S. L. Sorensen, F. Gel'mukhanov, A. Baev, and H. Ågren, Phys. Rev. Lett. **91**, 213003 (2003).
[15] P. Sałek, A. Baev, F. Gel'mukhanov, and H. Ågren, Phys. Chem. Chem. Phys. **5**, 1 (2003).
[16] F. Gel'mukhanov, V. Kimberg, and H. Ågren, Chem. Phys. **299**, 253 (2004).
[17] H. Ohashi, E. Ishiguro, Y. Tamenori, H. Kishimoto, M. Tanaka, M. Irie, T. Tanaka, and T. Ishikawa, Nucl. Instrum. Methods Phys. Res. A **467-468**, 529 (2001).
[18] H. Ohashi, E. Ishiguro, Y. Tamenori, H. Okumura, A. Hiraya, H. Yoshida, Y. Senba, K. Okada, N. Saito, I. H. Suzuki, K. Ueda, T. Ibuki, S. Nagaoka, I. Koyano, and T. Ishikawa, Nucl. Instrum. Methods Phys. Res. A **467-468**, 533 (2001).
[19] T. Tanaka and H. Kitamura, Nucl. Instrum. Methods Phys. Res. A **364**, 368 (1995); J. Synchrotron Radiat. **3**, 47 (1996).
[20] Y. Shimizu, H. Ohashi, Y. Tamenori, Y. Muramatsu, H. Yoshida, K. Okada, N. Saito, H. Tanaka, I. Koyano, S. Shin, and K. Ueda, J. Electron Spectrosc. Relat. Phenom. **63**, 114 (2001).
[21] N. Saito, K. Ueda, M. Simon, K. Okada, Y. Shimizu, H. Chiba, Y. Senba, H. Okumura, H. Ohashi, Y. Tamenori, S. Nagaoka, A. Hiraya, H. Yoshida, E. Ishiguro, T. Ibuki, I. H. Suzuki, and I. Koyano, Phys. Rev. A **62**, 042503 (2000).
[22] M. Domke, C. Xue, A. Pushmann, T. Mandel, E. Hudson, D. A. Shirley, and G. Kaindl, Chem. Phys. Lett. **173**, 122 (1990); **174**, 668(E) (1990).
[23] C. Pan and H. P. Kelly, Phys. Rev. A **39**, 6232 (1989).
[24] D. W. Lindle, L. J. Medhurst, T. A. Ferrett, P. A. Heimann, M. N. Piancastelli, S. H. Liu, D. A. Shirley, T. A. Carlson, P. C. Deshmukh, G. Nasreen, and S. T. Manson, Phys. Rev. A **38**, 2371 (1988).
[25] D. A. Shaw, G. C. King, D. Dvajanovic, and F. H. Read, J. Phys. B **17**, 2091 (1984).
[26] Y. Ma, C. T. Chen, G. Meigs, K. Randall, and F. Sette, Phys. Rev. A **44**, 1848 (1991).
[27] H. M. Köppe, B. Kempgens, A. L. D. Kilcoyne, J. Feldhaus, and A. M. Bradshaw, Chem. Phys. Lett. **260**, 223 (1996).
[28] H. Ågren and R. Arneberg, Phys. Scr. **30**, 55 (1984).
[29] W. C. Stolte, D. L. Hansen, M. N. Piancastelli, I. Dominguez Lopez, A. Rizvi, O. Hemmers, H. Wang, A. S. Schlachter, M. S. Lubell, and D. W. Lindle, Phys. Rev. Lett. **86**, 4504 (2001).
[30] E. Shigemasa, T. Hayaishi, T. Sasaki, and A. Yagishita, Phys. Rev. A **47**, 1824 (1993).
[31] P. Baltzer, M. Lundqvist, B. Wannberg, L. Karlsson, M. Larsson, M. A. Hayes, J. B. West, M. R. F. Siggel, A. C. Parr, and J. L. Dehmer, J. Phys. B **27**, 4915 (1994).
[32] P. Sałek, F. Gel'mukhanov, H. Ågren, O. Björneholm, and S. Svensson, Phys. Rev. A **60**, 2786 (1999).
[33] R. Kosloff, J. Phys. Chem. **92**, 2087 (1988).
[34] P. Sałek, F. Gel'mekhanov, and H. Ågren, Phys. Rev. A **59**, 1147 (1999).
[35] B. Huron, J.-P. Malrieu, and P. Rancurel, J. Chem. Phys. **58**, 5745 (1973).
[36] C. Angeli and M. Persico, Theor. Chem. Acc. **98**, 117 (1997).
[37] T. H. Dunning, Jr., J. Chem. Phys. **55**, 716 (1971).
[38] Paweł Sałek, Comput. Phys. Commun. **150**, 85 (2003).
[39] S. K. Botting and R. R. Lucchese, Phys. Rev. A **56**, 3666 (1997).